

# Low Temperature Phase Transition in $\text{Sr}_{0.66}\text{Ba}_{0.34}\text{Nb}_2\text{O}_6$ Single Crystal Fibers

J. L. B. Faria,\* C. W. A. Paschoal, P. T. C. Freire, A. P. Ayala,  
F. E. A. Melo, J. Mendes Filho,  
*Departamento de Física, Universidade Federal do Ceará, Caixa Postal 6030,  
60455-760 Fortaleza, Ceará, Brazil*

I. A. Santos, J. A. Eiras  
*Departamento de Física, Universidade Federal de São Carlos, Caixa Postal 676,  
13565-670 São Carlos, São Paulo, Brazil*  
(April 26, 2024)

The structural changes in  $\text{Sr}_{0.66}\text{Ba}_{0.34}\text{Nb}_2\text{O}_6$  single crystal fibers when the temperature decreases from 295 to 10 K is investigated by dielectric constant measurements and Raman spectroscopy. The anomaly observed in the plot of  $\epsilon''$  is associated to the variation in the intensity and frequency of some Raman modes. We observe that the intensity of some low energy modes has a very singular behavior for the  $y(xz)\bar{y}$  scattering geometry. In the high energy region ( $> 850 \text{ cm}^{-1}$ ), a band at  $\sim 880 \text{ cm}^{-1}$  disappears when the temperature is cooled down to 10K for the  $y(xz)\bar{y}$  geometry and shifts to higher energy values for the  $y(zz)\bar{y}$  geometry.

## I. INTRODUCTION

Strontium barium niobate  $\text{Sr}_x\text{Ba}_{1-x}\text{Nb}_2\text{O}_6$  (SBN) is a ferroelectric system with remarkable electro-optic properties. Thin films have been used in optical data-storage [1], microelectronic devices applications and crystalline and amorphous substrates [2,3]. Beside its technological applications, SBN exhibits interesting structural characteristics as incommensurate superstructures [4], polarization memory [5] and high stability to intense laser radiation source [6]. Raman spectroscopy has been employed to study the variation of the vibrational modes of SBN in connection to its ferroelectric characteristics [7,8].

From the studies performed in the late 60's, it is known that the room temperature crystalline structure of SBN belongs to the "tungsten-bronze" family, whose the main compound is  $\text{K}_x\text{WO}_3$ . Since the sites of this structure are not completely filled, a large variety of compositional formulas is found in the literature [9]. Compounds of SBN with  $x$  ranging from 0.25 up to 0.75 (the range of stability for the solid solution [10,11]) were studied by Jamieson *et. al.* [9].

There are some evidences of the existence of one or two phase transitions in these bulk compounds when the temperature is lowered down to 10 K [12,13]. The techniques employed were X-ray diffraction, specific heat and pyroelectric coefficient measurements in these references. Although Raman spectroscopy study has been used to investigate the ferroelectric-paraelectric transition in SBN occurring for  $T > 300 \text{ K}$  [14], no one has employed this technique to investigate the phase transitions occurring for  $T < 300 \text{ K}$ . We address here the phase transition undergone by SBN ( $x=0.66$ ) at about 80 K as observed both

by Raman spectroscopy and dielectric constant measurements giving an additional evidence via optical measurements for a phase transition undergone by SBN crystal fibers at low temperatures.

## II. EXPERIMENTAL

The SBN samples used in the experiments were prepared using the standard oxide mixture route. Ceramic powders with nominal composition  $(\text{Sr}_{0.61}\text{Ba}_{0.39})\text{Nb}_2\text{O}_6$  - SBN 61/39 were prepared beginning from the mixture of  $\text{Nb}_2\text{O}_5$ ,  $\text{Ba}(\text{NO}_3)_2$  and  $\text{SrCO}_3$  in the wanted proportions. The precursory powders were mixed in a ball milling during 3 hours for homogenization, being after calcined for solid state reaction which takes place at  $1300 \text{ }^\circ\text{C}$  during 3 hours. The samples were compacted to form a disk shape sample. Finally, the disks (with the dimensions  $25 \times 12 \times 1 \text{ mm}^3$ ) were fired at a sintering temperature of  $1350 \text{ }^\circ\text{C}$  during 3.5 hours. Sticks (with  $20 \times 0.7 \times 0.7 \text{ mm}^3$ ) were cut of the sintering plates for the growth of the monocrystalines fibers by using the fusion technique with laser (LHPG - Laser Heated Pedestal Growth). In this technique the ceramic sticks are used as seeds for the growth of the fibers. The composition of the fibers of pure SBN nominally indicated that everybody was faulty in Ba. The analysis were made through an EDX microprobe in an electronic microscope Zeiss DSM-960, that revealed fibers with nominal composition Sr/Ba 61/39 present the value 66/34.

The Raman spectra were recorded with a Jobin Yvon T64000 spectrometer, equipped with a  $\text{N}_2$ -cooled Charge Coupled Device (CCD) detection system. The

\*Author to whom correspondence should be addressed: e-mail: hulk@fisica.ufc.br

slits were set for a  $2 \text{ cm}^{-1}$  spectral resolution. The line  $514.5 \text{ nm}$  of an Argon ion laser was used as excitation. A Olympus microscope lens with a focal distance  $f = 20.5 \text{ mm}$  and numeric aperture  $\text{NA} = 0.35$  was used to focus the laser to sample surface. The incident power density was of the order of  $100 \text{ W/cm}^2$ . Several measurements were performed in the temperature range investigated and carried out in the  $y(zz)\bar{y}$  and  $y(xz)\bar{y}$  scattering geometries [15], where x,y and z are associated to the crystallographic axis.

### III. RESULTS AND DISCUSSION

The dielectric constant is an ideal parameter to describe the electric properties of dielectric materials [16]. For most of the materials the dielectric constant in the linear regime is not a function of the applied electric field intensity, but for alternate fields, it will depend on frequency. Fig. 1 displays both the real ( $\epsilon'$ ) and the imaginary ( $\epsilon''$ ) parts of dielectric constant as a function of temperature. The dielectric constant of SBN is characterized by two different features. The most intense is called  $\alpha$  which appears in the inset of Fig.1 for  $T \approx T_c$ , the Curie temperature. Such an anomaly has its origin on the temperature and frequency dependence of the dielectric permittivity of ferroelectrics with relaxor character near the ferroelectric - paraelectric phase transition [13]. We will not attempt to discuss this  $\alpha$  - feature because it is well studied elsewhere [13]. Rather, we will put forward considerations about another very important characteristic in Fig. 1. The second feature of interest is the  $\gamma$  anomaly which can be associated with polarization fluctuation originating from the relaxor nature of SBN solid solution [17]. This means that SBN, like  $\text{Pb}_{1-x}\text{Ba}_x\text{Nb}_2\text{O}_6$ , is a different type of relaxor ferroelectric where the conventional dipolar model is no valid anymore [18]. For SBN we must consider both local and macroscopic polarization states, where the former differ slightly from the latter. The two possible local states are separated by an energy barrier in the energy well. At high temperatures these barriers can be overcome due to thermal energy. However, for low temperatures the activation barrier is comparable to the thermal energy allowing relaxation processes through changes in the polarization states.

Another interpretation for the  $\gamma$  anomaly is a diffuse phase transition undergone by SBN crystal fiber at  $80 \text{ K}$ . This interpretation is established by the work of Ref. [12] where spontaneous polarization, pyroelectric coefficient and dielectric constant measurements performed on  $\text{Sr}_{0.5}\text{Ba}_{0.5}\text{Nb}_2\text{O}_6$  crystal bulk point to a phase transition between  $60$  and  $80 \text{ K}$ . Therefore, it is plausible to expect that this anomaly observed in SBN crystal fibers should be due to a phase transition undergone by the material.

In Figs. 2 and 3 we display the Raman scattering spectra in the low frequency region at several temperatures recorded in the  $y(zz)\bar{y}$  and  $y(xz)\bar{y}$  scattering geometries, respectively. At the lowest temperature, 8 bands are observed. Increasing the temperature, these bands become broader due to anharmonic effects [19]. Apparently, no change is observed. However, if one normalizes all bands to that at  $106 \text{ cm}^{-1}$  (band 2), it can be seen that the intensity of the band at  $75 \text{ cm}^{-1}$  (band 1) changes abruptly around  $85 \text{ K}$ , as shown in Fig 4. In this plot the background was properly subtracted [20,21]. Here we arrive to an important point: the sudden intensity change of a low frequency band. The significance of this variation is discussed as follows.

The intensity of a phonon results from different factors as, for example, a deformation potential interaction term [22]. This can be associated to a change of structure when the material is being subjected to a variation of external condition, e.g., temperature or pressure. Changes in the intensities of low-frequency Raman bands evidencing phase transition by temperature variation were already reported for a well known ferroelectric crystal, triglycine sulfate, where a phonon of  $60 \text{ cm}^{-1}$  was connected with the onset of the phase transition [23]. By pressure variations, it was also observed change of structure through the study of intensity of Raman bands [24,25]. In the first case, abrupt changes of intensity in several bands in the spectra taken place between  $2.03$  and  $2.24 \text{ GPa}$  provided strong evidence that modifications in the unitary cell of the crystal happened in this pressure interval. In the second case one striking change in the relative intensities of bands associated to modes of  $41$  and  $48 \text{ cm}^{-1}$  is verified for pressures between  $2.2$  and  $2.3 \text{ GPa}$ . An additional low energy band appears in the Raman spectra evidencing a phase transition is present [25]. However, changes in the relative intensity of Raman bands with variation of any thermodynamic parameter does not imply, necessarily, a phase transition has occurred. These variations sometimes may be associated to the internal reordering of ions in the unit cell but with no change of structure; one example is given by  $\text{LiNa}_3(\text{SO}_4)_2 \cdot 6\text{H}_2\text{O}$  crystal, where great modifications in the Raman intensities occurring when temperature changes from  $12$  to  $300 \text{ K}$  are not associated with any phase transition [26]. In the case of SBN crystal fibers here investigated we believed that the change in the Raman intensities may be credited to a phase change, because, as was already shown, measurements of dielectric constant for the SBN crystal bulk point to the existence of a phase transition [12].

Fig. 5 shows the SBN Raman spectra in the spectral range  $760\text{-}930 \text{ cm}^{-1}$  taken from  $10$  to  $90 \text{ K}$  for the  $y(xz)\bar{y}$  scattering geometry. Bands in this region are due to  $\nu_1$  modes of the  $\text{NbO}_6$  structure [27]. As observed by other authors [14] this region presents an extremely broad band whose rising is possibly associated to a struc-

tural disorder. In the structure there exist octahedra of  $\text{NbO}_6$  with the polar direction close to the O – Nb – O axis. These axes are not exactly parallel to the c axis and, additionally, since we have two non-equivalent Nb ions, this give rise to two slightly different  $\nu_1$  vibrations of the  $\text{NbO}_6$  structure. Starting from 90 K, the intensity of the band at  $880 \text{ cm}^{-1}$  decreases progressively down to 20 K, when the band disappears completely. As the origin of these two bands is associated with structural disorder, this means that for low temperatures a new configuration is being supplied to  $[\text{NbO}_6]^{7-}$  ions. This new configuration may be originated either by a change in SBN unitary cell as a consequence of the temperature variation or by a local change of the neighboring region of the ion.

In Fig. 6 we show the  $\nu_1$  mode region for the  $y(zz)\bar{y}$  scattering geometry. Two bands are also observed. Decreasing the temperature, the intensity of the higher energy band decreases but, instead of disappearing completely, it remains even at 10 K. When looked carefully around 50 K, the energy of the band with higher Raman shift undergoes a jump. The arrows placed in spectra of 50 K and 10 K show the exact value of the center of the bands obtained by lorentzians fittings. By one hand, the fact that the two bands are present down to the lowest temperature in this different scattering geometry means that the two non-equivalent  $\text{NbO}_6$  structures remains down to 10 K. On the other hand, a jump in the energy of one band is pointing to a change of the neighboring around the octahedral  $[\text{NbO}_6]^{7-}$  ion. Moreover, the fact that some variation of band intensities of external modes are also being observed serves as a guide when deciding on the conclusion to be adopted, in our case, the existence of a structural phase transition.

As summary, through Raman spectroscopy and dielectric constant measurements it was possible to verify the existence of a phase transition for SBN crystal fibers at temperatures below 100 K. The evidences are: (i) changes in relative intensities of low energy bands; (ii) disappearance of a high energy band, associated with the ion  $[\text{NbO}_6]^{7-}$  vibration in the  $y(xz)\bar{y}$  scattering geometry and abrupt change in energy of the same phonon in the  $y(zz)\bar{y}$  scattering geometry; (iii) change in dielectric constant in the same temperature limits where occur the variations in the low energy modes.

**Acknowledgments** - J. L. B. Faria and C.W.A. Paschoal acknowledge financial support from CNPq and FUNCAP, respectively. P. T. C. Freire wishes to acknowledge the financial support from FUNCAP through a grant No . 017/96 P&D. The authors acknowledge A.C. Hernandez for the fiber growth and A. G. Souza Filho and I. Guedes for discussions related to this work. Financial support from CNPq, FAPESP and FINEP is also gratefully acknowledged.

- [1] J. P. Wilde et. al., *Opt. Lett.*, **17**, 853 (1992)
- [2] R. E. Youden et. al., *Ferroelectric Thin Film IV Symposium*, 173 (1995).
- [3] R. G. Mendes, E. B. Arajo, H. Klein and J. A. Eiras, *Bol. Soc. Esp. Ceram. V.*, **38**, 455 (1999).
- [4] L. A. Bursill and P. J. Lin, *Acta Crystallogr., Sect B* **43**, 49 (1987)
- [5] A. M. Glass, *J. Appl. Phys.* **40**, 4699 (1969)
- [6] P. B. Jamieson, S. C. Abrahams, J. L. Bernstein, *J. Chem. Phys.* **50**, 4352 (1969)
- [7] R. Clarke and D. Siapkas, *J. Phys. C* **8**, 337 (1975)
- [8] G. Burns, J. D. Axe and D. F. O’Kane, *Solid State Commun.* **7**, 933 (1969)
- [9] P. B. Jamieson, S. C. Abrahams and J. L. Bernstein, *J. Chem. Phys.* **48**, 5048 (1968).
- [10] A. A. Ballman and H. Brown, *J. Cryst. Growth*, **1** 311 (1967).
- [11] P. V. Lenzo, E. G. Spencer, and A. A. Ballman, *Appl. Phys. Letters*, **11**, 23 (1967).
- [12] Y. Xu, Z. Li, H. Wang, H. Chen *Phys. Rev. B*, **40**, 11902 (1989).
- [13] H. Fan, L. Zhag, X. Yao, *J. Mat. Sci.*, **33**, 895 (1998).
- [14] R. E. Wilde, *J. Raman Spectrosc.* **22**, 321-325 (1991).
- [15] T. C. Damen, S. P. S. Porto, B. Tell, *Phys. Rev.*, **142**, 570 (1966).
- [16] H. Fröhlich, *Theory of Dielectrics-Dielectrics constants and Dielectrics loss*, 2nd. ed. Oxford University Press, Oxford (1958).
- [17] In fact, in some experiments a third feature called  $\beta$  - anomaly is also observed and it was pointed as an additional experimental evidence for the incommensurate superlattice structure of SBN ceramic. This incommensurate - commensurate phase transition was reported by the work of L. A. Bursill, and P.J. Lin, *Philos. Mag. B*, **54**, 157 (1986) as occurring at about - 75 °C in the SBN ( $x = 0.5$ ) single crystal.
- [18] R. Guo, A. S. Bhalla, C. A. Randall and L. E. Cross, *J. Appl. Phys.*, **67**, 6405 (1990).
- [19] N. W. Ashcroft, N. D. Mermin, *Solid State Physics*, Saunders College, 1976, Cap 25.
- [20] S. S. Bukalov and L. A. Leites, *Opt. Spectrosc.*, **56**, 6 (1984).
- [21] D. I. Ostrovskii, A. M. Yaremko, and I. P. Vorona, *J. Raman Spectrosc.*, **28**, 771 (1997).
- [22] R. Loudon, *Advan. Phys.*, **13**, 423 (1964).
- [23] E. Silberman, S.H. Morgan, J.M. Springer, *J. Raman Spectrosc.* **10**, 248 (1981).
- [24] B. L. Silva, PhD *Thesis*, UFC 1997.
- [25] A. M. R. Teixeira, P. T. C. Freire, A. J. D. Moreno, J. M. Sasaki, A. P. Ayala, J. Mendes Filho, F. E. A. Melo, *Solid State Commun.* **116**, 405 (2000).
- [26] J. Mendes Filho, R. O. Paiva, P. T. C. Freire, F. E. A. Melo, I. Guedes, J. M. Sasaki, E. E. Castellano, J. Zukerman-Schpector, *J. Raman Spectrosc.*, **30**, 289 (1999).
- [27] H. R. Xia, H. C. Chen, H. Yu, K. X. Wang, and B. Y. Zhao, *Phys. Stat. Sol. (b)*, **210**, 47 (1998).

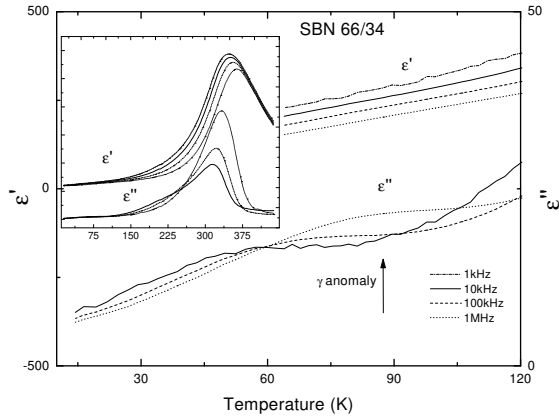


FIG. 1. Plot temperature *vs.* dielectric constants  $\epsilon'$  and  $\epsilon''$  of the SBN 66/34 for temperatures between 10 and 450K.

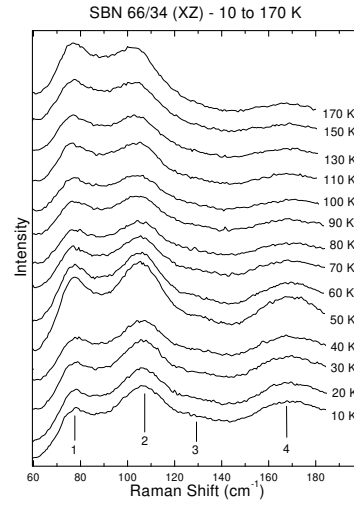


FIG. 3. Raman spectra of SBN 66/34 in the scattering geometry  $y(xz)\bar{y}$  for temperatures between 10 and 170 K.

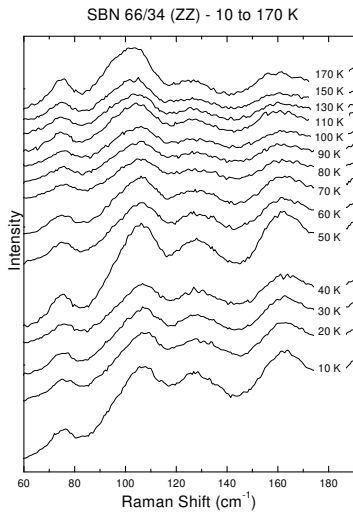


FIG. 2. Raman spectra of SBN 66/34 in the scattering geometry  $y(zz)\bar{y}$  for temperatures between 10 and 170 K.

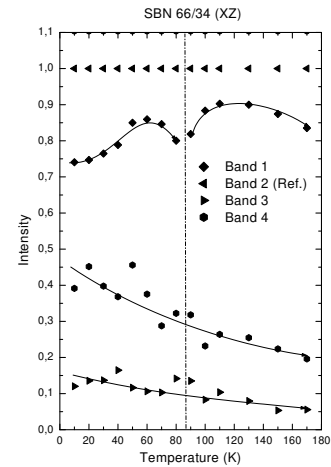


FIG. 4. Plot intensity normalized *vs.* temperature of SBN 66/34 in the scattering geometry  $y(xz)\bar{y}$  for temperatures between 10 and 170 K.

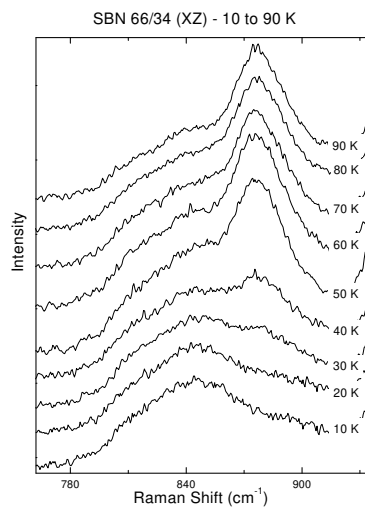


FIG. 5. Raman spectra of SBN 66/34 in the scattering geometry  $y(xz)\bar{y}$  for temperatures between 10 and 90 K.

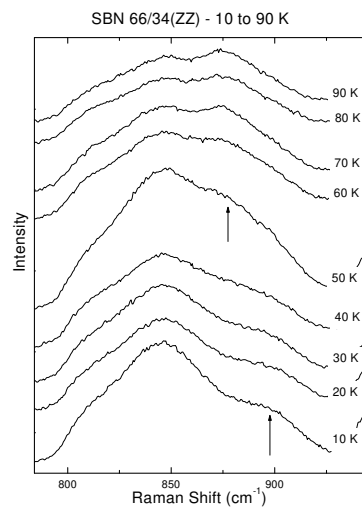


FIG. 6. Raman spectra of SBN 66/34 in the  $y(zz)\bar{y}$  scattering geometry for temperatures between 10 and 90 K. The arrow indicates the center of the band with the highest energy.